NOAA Technical Memorandum ERL ARL-166

HYBRID SINGLE-PARTICLE LAGRANGIAN INTEGRATED TRAJECTORIES (HY-SPLIT): MODEL DESCRIPTION

Roland R. Draxler

Air Resources Laboratory
Silver Spring, Maryland
September 1988

UNITED STATES DEPARTMENT OF COMMERCE

C.William Verity
Secretary

NATIONAL OCEANIC AND ATMOSPHERIC ADMINISTRATION

William E. Evans
Under Secretary for Oceans and Atmosphere/Administrator

Environmental Research Laboratories

Vernon E. Derr,
Director

NOTICE

Mention of a commercial company or product does not constitute an endorsement by NOAA Environmental Research Laboratories. Use for publicity or advertising purposes of information from this publication concerning proprietary products or the tests of such products is not authorized.

For sale by the National Technical Information Service, 5285 Port Royal Road
Springfield, VA 22161

CONTENTS

HYBRID SINGLE-PARTICLE LAGRANGIAN INTEGRATED TRAJECTORIES (HY-SPLIT): MODEL DESCRIPTION

Roland R. Draxler

ABSTRACT. The algorithms and equations used in the development of a long-range transport and dispersion model are presented. The model calculation methods are a hybrid between Eulerian and Lagrangian approaches. A single pollutant particle represents the initial source. Advection and diffusion calculations are made in a Lagrangian framework. However, meteorological input data can either be gridded from rawinsonde observations or archived from the output of an Eulerian primitive equation forecast model. As the dimensions of the initial particle diffuse into regions of different wind direction or speed, the single particle is divided into multiple particles to provide a better representation of the more complex flow field. Air concentrations are calculated on a fixed three-dimensional grid by integrating all particle masses over the sampling time.

1. INTRODUCTION

The development of the HY-SPLIT long-range transport (LRT) calculation technique has evolved in several stages, from a simple wind-shear induced particle dispersion study (Draxler and Taylor, 1982), to the inclusion of air concentration calculations with only a day/night mixing assumption (Draxler, 1982), to the calculation of vertical mixing coefficient profiles and vertical particle motions (Draxler, 1987). At this stage the model development has sufficiently matured to justify a more complete description of some of the algorithms and equations. The modeling technique is in many ways similar to particle-in-cell (PIC) methods (Lange, 1978) with the exception that one starts with a single particle that may split into as many particles as needed to describe the pollutant distribution. This approach requires special numerical techniques to limit the number of particles. These methods are discussed in more detail in section 2.4.

Although each particle has an associated horizontal and vertical diffusive component, similar to a "puff" model, the subsequent particle division determines the spatial and temporal concentration distributions, rather than the diffusion about any one particle. This contrasts with PIC methods, where initially the concentration distribution is defined by the particles, but at later times there may be too few particles in adjacent cells to define the concentration field without assuming a particle probability distribution.

In most dispersion models, the limiting feature is the meteorological data used in the calculations. In previous model versions rawinsonde observations were the only data source. These data were gridded on a user-selected polar stereographic grid by a preprocessor program. This was the method used when the dispersion model calculations were compared with the air concentrations measured during the Cross Appalachian Tracer Experiment (CAPTEX) (Draxler, 1987; Draxler and Stunder, 1988). The HY-SPLIT revision permits the use of meteorological input data from other sources, in particular meteorological data fields archived from the National Weather Service's (NWS) Nested Grid Model (NGM) (Phillips, 1975). NGM data can be archived from the model by the Air Resources Laboratory (ARL) at various intervals and grids (hourly to 6 hourly and 85 to 190 km).

2. MODEL OVERVIEW

Conceptually the LRT calculation can be divided into several elements that represent the major processes that must be modeled. These elements include (1) the pollutant source and its subsequent division (particle generation), (2) particle advection, (3) vertical and horizontal mixing, (4) particle merging to limit computational expense, and (5) air concentration calculations. These processes are linked as shown on the "flowchart" in Table 1 and occur within a loop representing the integration time step.

Table 1. "Flowchart" of model calculations during each time step

ROUTINE	CALCULATION
INPUT	Input meteorological data appropriate for the time step
SOURCE	Emit one particle at origin (X,Y,Z) for each time step for a continuous source or only once for an instantaneous source
V-SPLIT	Split a particle in two if its vertical extent covers at least two layers
MERGE	Combine the masses of adjacent particles of the same age that occur within the same vertical layer
H-SPLIT	Split a particle into four if its horizontal extent covers two grid cells
ADVECT	Calculate the advection, and horizontal and vertical diffusion for each particle
SUM MASS	Integrate the mass contribution of each particle to the concentration grid

Of course there are many other routines required to complete the model, including entering various parameters, initializing arrays, producing output maps of particle positions and concentrations, and other diagnostic procedures.

2.1 Advection

Each particle is identified by its mass Q, horizontal position in grid coordinates X,Y, height above model terrain Z, horizontal σ_h and vertical σ_v standard deviations of its position. When P represents the horizontal position vector of a particle at X,Y, the horizontal advection of the particle from P_0 to P_2 over the time step Δt is computed by the process

$$P_2 = P_0 + (V_0 + V_1)\,\Delta t/2,$$

where V_0 is the horizontal wind vector at the initial position P_0 and V_1 is the wind at position

$$P_0 + V_0 \Delta t.$$

This method is a simple first-order approximation to account for curvature in the wind field. The wind vectors V_0 and V_1 are defined at the data level nearest to the initial vertical particle height Z_0. The new vertical height of the particle is given by

$$Z_2 = Z_0 + (W_0 + W_1)\ \Delta t/2.$$

The vertical velocity W_1 is defined at the same position as V_1. A bilinear interpolation from the data grid is used to define meteorological variables at the particle position.

2.2 Horizontal and Vertical Diffusion

Because each particle represents a growing cluster of particles as represented by the uncertainty in the particle's position, one can define those dimensions using the conventional notation of the standard deviation of the particle position in the horizonal σ_h and vertical σ_v directions. The rate of horizontal growth

$$d\sigma_h/dt = 1853$$

is constant (Heffter, 1965), where σ_h is in meters and t in hours. However, the vertical growth rate depends upon the local vertical diffusivity profile K_z computed from the meteorological data:

$$(d\sigma_v)^2/dt = 2\ K_z.$$

Although this relationship was considered valid primarily during stable conditions (Hunt, 1985), the values of K_z are so large during unstable conditions that the exact form of the equation is less important.

The particle, with its associated standard deviations for computational purposes, can be considered as a cylinder. Because the exact distribution of particles within that cylinder is quite uncertain, the distribution is assumed to be uniform. The diffusion equations were initially defined for Gaussian distributions; therefore one must use the relationship between the Gaussian and uniform distribution, as shown on Fig. 1. At 1.54 σ, the ordinate of the Gaussian distribution is equal to the average value of the distribution; that is the areas above and below the horizontal dashed lines are equal. With this relationship, the horizontal radius R of the cylinder becomes 1.54 σ_h and the vertical height H equals 3.08 σ_v.

The horizontal growth is assumed to be unbounded, but the vertical growth is limited by the ground and the top of the boundary layer. If a particle is above the boundary layer (Z_{bl}), it will continue to move and diffuse as particles below Z_{bl}. However, eventually it could mix out of the top of the model domain (Z_{mt}). A fraction of the particle's mass

$$(Z_{mt} - Z_{cb})/(Z_{ct} - Z_{cb})$$

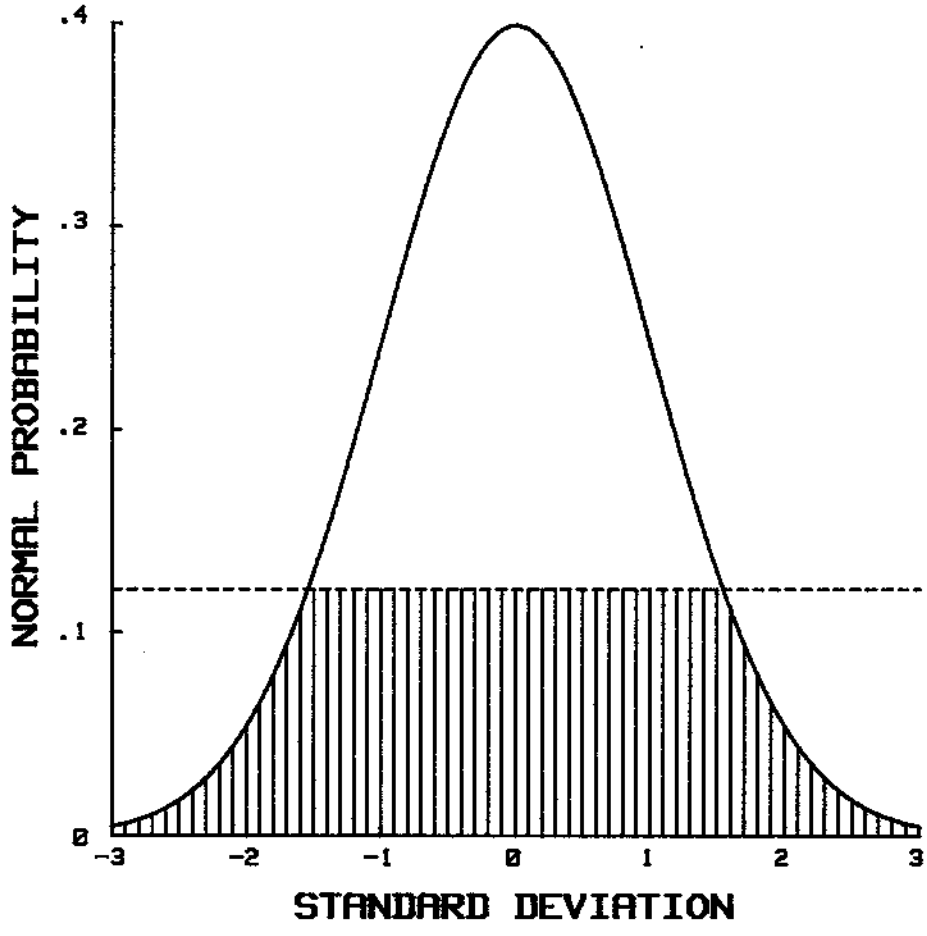

Figure 1. Normal probability distribution. The dashed horizontal line indicates the ordinate value at which the shaded area equals the area above the line at 1.54 σ.

remains within the model each time step when $Z_{ct} > Z_{mt}$. The remainder is lost. The subscripts denote the heights of the cylinder top (ct) and bottom (cb). Note that the denominator must equal 3.08 σ_v or

$$Z_{ct} = Z + 1.54\ \sigma_v$$

and

$$Z_{cb} = Z - 1.54\ \sigma_v.$$

The vertical distribution σ_v is redefined for particles with Z above Z_{bl} when Z_{ct} exceeds Z_{mt} or Z_{cb} is below Z_{bl}; or for particles with Z below Z_{bl} when Z_{ct} is above Z_{bl} or Z_{cb} is below zero. In those cases the new σ_v is redefined by

$$\sigma_v = (Z_{ct} - Z_{cb})/3.08,$$

using the new cylinder heights Z_{ct} and Z_{cb} where Z_{ct} is redefined at Z_{bl} or Z_{mt}, and Z_{cb} at 0 or Z_{bl} for particles below or above Z_{bl}, respectively.

Particles at heights that exceed Z_{mt} are dropped from the calculation. Because Z_{bl} can change with the meteorology, particles above Z_{bl} can at later times be below Z_{bl}. If Z_{bl} exceeds Z_{mt}, a condition that should be avoided by defining Z_{mt} well above the domain of interest, a large mass loss could occur through vigorous mixing out of the model top.

2.3 Particle Division

When the growth of the cylinder extends either vertically or horizontally over two or more meteorological data points, then a single particle position can no longer adequately represent the advection-diffusion process. At this stage a particle is divided into two or more particles in which the sum of their masses equals the mass of the initial particle. In the vertical dimension this process can be described as shown in Fig. 2. Here the meteorological layers are shown by the long dashed lines. The sigma surface (discussed in section 3), where the meteorological parameters are calculated, is defined at the layer midpoint. When the growth of the cylinder is large enough to fully encompass at least two layers, that is Z_{ct} extends past Z_3 and Z_{cb} is below Z_1, then the particle Q_0 is divided into two particles of mass

$$Q_2 = Q_0\ (Z_2 - Z_1)/(Z_3 - Z_1)$$

and

$$Q_3 = Q_0\ (Z_3 - Z_2)/(Z_3 - Z_1).$$

The new particles Q_2 and Q_3 have the same horizontal position as Q_0 but have an elevation equal to the layer midpoint. The σ_h value remains the same but the new σ_v value is proportioned exactly the same way as the mass.

The horizontal growth continues until the cylinder radius R is greater than the grid spacing G. At this point (Fig. 3) the particle is divided into four new particles, each with 0.25 of the initial mass. The new positions are orthogonal and equidistant from the old position by 0.5 R, with a σ_h value of 0.5 of the initial value but with the same σ_v value. The horizontal division is not important until longer travel times; given the constant growth rate, it would take 33 h for the first horizontal split to occur on a 85-km grid and 68 h on a 190-km grid.

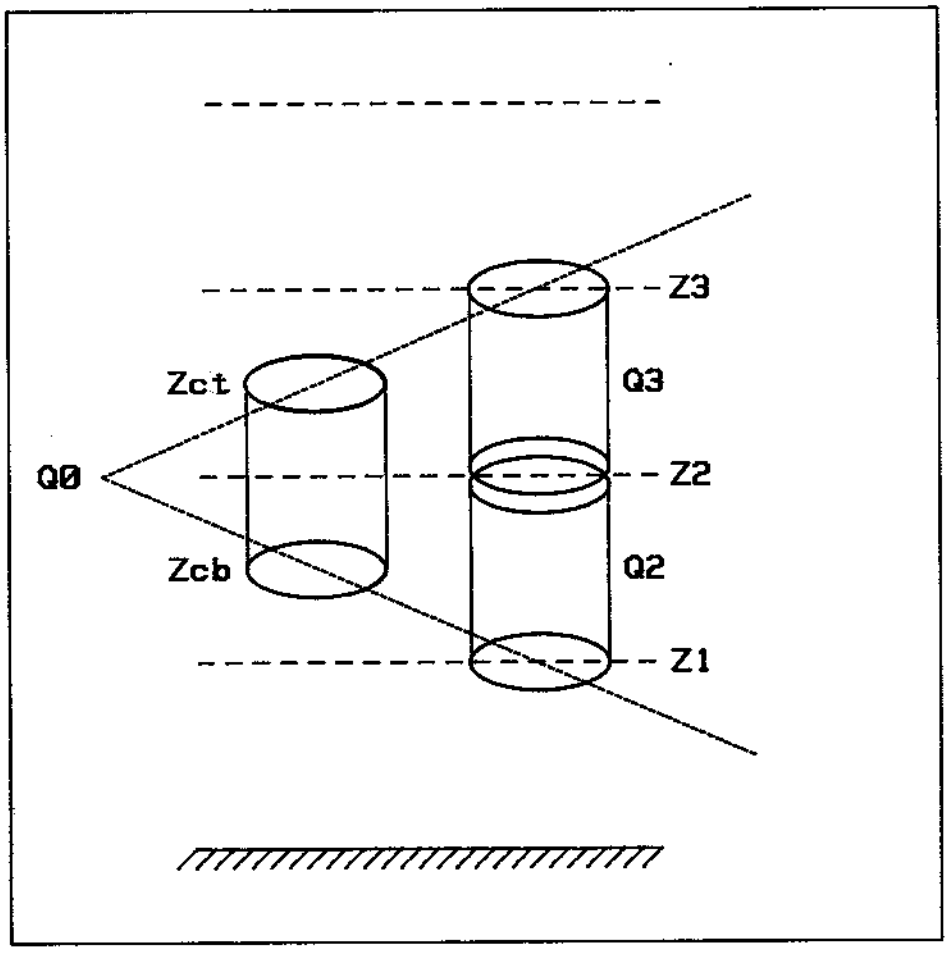

Figure 2. Illustration of how a single particle Q_0 splits due to vertical diffusion into two particles Q_2 and Q_3.

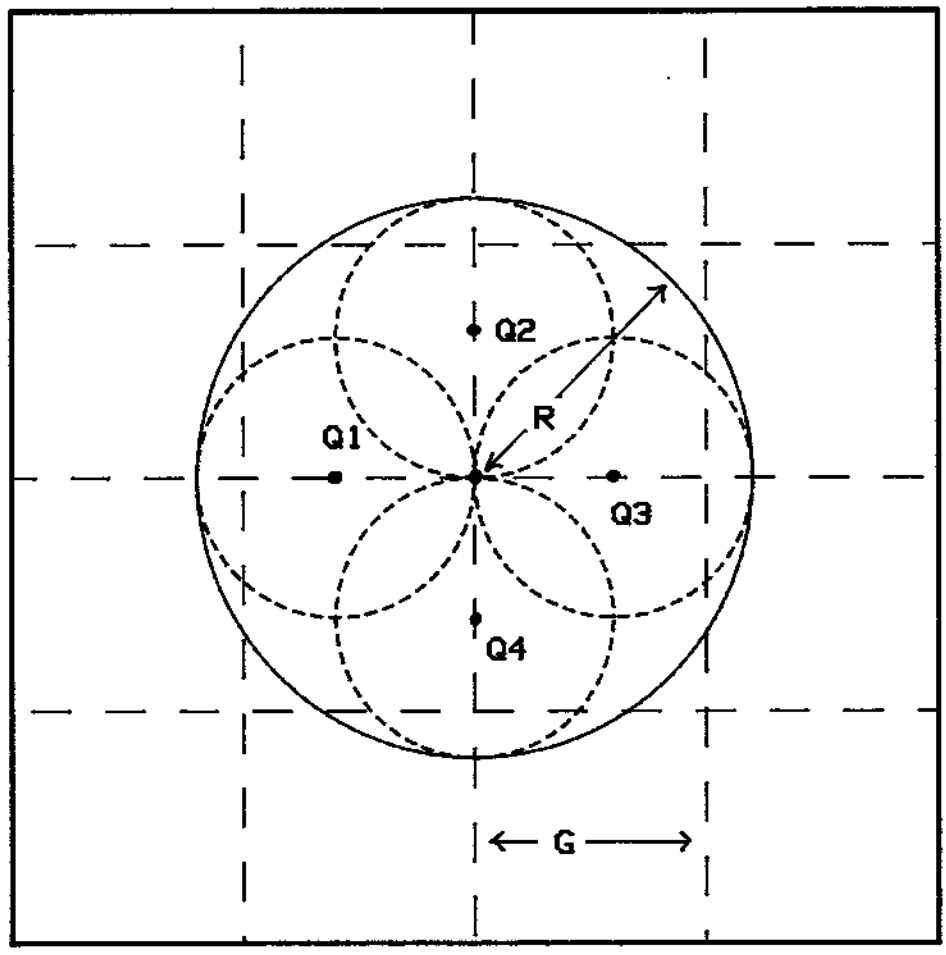

Figure 3. Illustration of how a single particle with radius R splits due to horizontal diffusion into four particles (Q_1, Q_2, Q_3, and Q_4) each with radius R/2.

2.4 Particle Convergence

The key element to the practical application of this model is the elimination of duplicate particles, because the generation of new particles, especially due to vertical diffusion, can quickly overwhelm even the fastest computer. Particles are merged only if they are of the same age (σ_h values are equal), they are within the same layer, and their respective cylinders overlap by some predefined value. For instance, particles 1 and 2 are merged as shown in Fig. 4, when the distance between their positions

$$|P_2 - P_1| \leq fR,$$

where f is a fraction of the distance R. The default value of f is 1.0 as in the example shown in Fig. 4. The merged particle at position P_3 then has these mass-weighted attributes:

$$P_3 = (Q_2 P_2 + Q_1 P_1)/(Q_2 + Q_1),$$

$$Q_3 = Q_2 + Q_1,$$

$$\sigma_{h3} = \sigma_{h2} = \sigma_{h1},$$

$$\sigma_{v3} = (Q_2\sigma_{v2} + Q_1\sigma_{v1})/(Q_2 + Q_1).$$

Although the merging of coincident particles is in itself rather a trivial computation, the process can be cumbersome because there are no limits to the number of particles that can be generated or to their ages. Further, the particle positions are stored more or less at random in a large one-dimensional array. To quickly identify which particles are clustered together in the array, the particle position array is first sorted by age, level, X position, and Y position. In this way nearby particles will be adjacent in the array. In addition, particles with a mass less than 10^{-15} of the initial particle mass are dropped. The sorting routine is quite efficient, requiring n passes through the array where 2^n equals the number of particles.

The particle merging occurs after the vertical diffusion division, thereby eliminating redundant particles at the same level. However, the horizontal division occurs after the merge calculation to avoid having a particle split and merge in the same time step.

2.5 Concentration Calculations

Air concentrations are computed from a sampling grid defined at one or more user-specified heights, which do not have to be coincident with the meteorological sigma levels, and on a horizontal grid that is either identical to or a multiple of the meteorological data grid. Each grid point is considered to be a sampling location, so that air concentrations are computed at that grid point, rather than as cell averages as in conventional Eulerian models. At grid point (i,j,k) the air concentration is

$$C_{i,j,k} = (\Delta t/T_a)\ (R/A)\ \sum_{1}^{T_a/\Delta t}\ \sum_{1}^{A/R}\ \sum_{1}^{p}\ \frac{Q}{\pi\ R^2\ H}$$

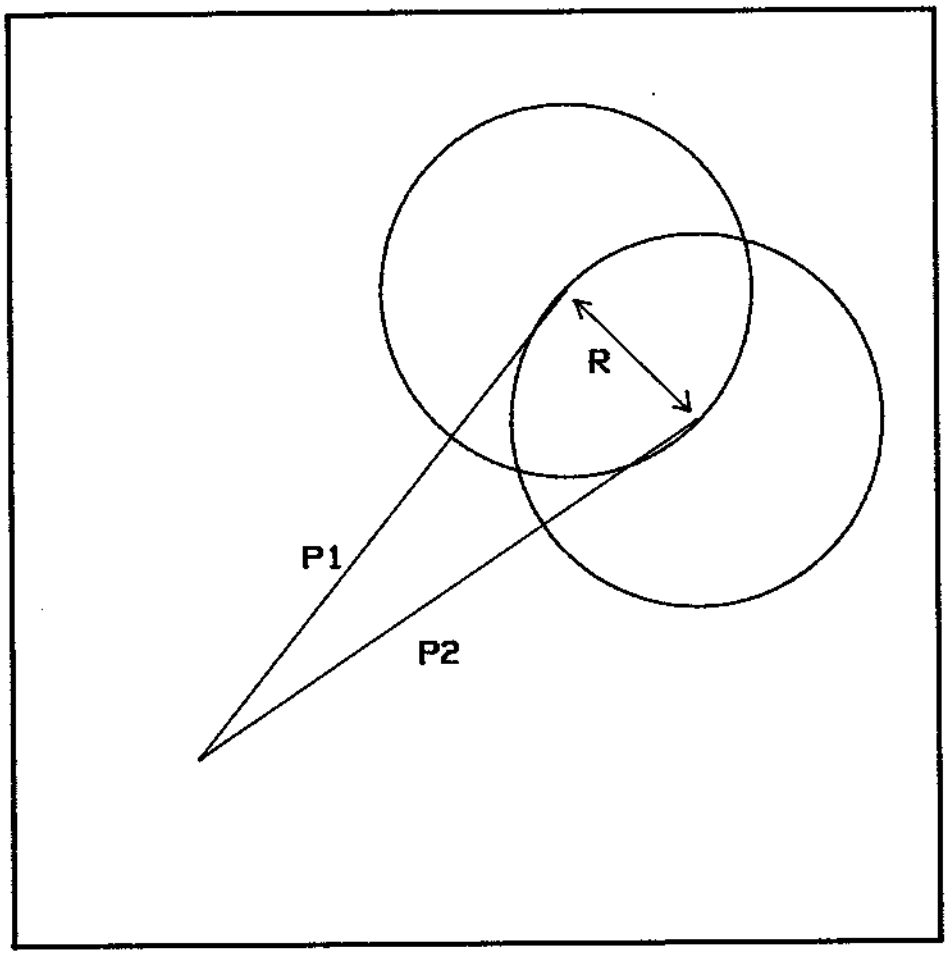

Figure 4. Illustration of when two particles are merged into a single particle. In this case it occurs when the difference between position vectors P_1 and P_2 is less than R.

where the sums are taken over $T_a/\Delta t$ intervals over the averaging time T_a; over A/R particle positions linearally interpolated over the distance advected (A) during the time step; and over p particles. In addition the cylinder radius R with height H must intercept the grid point both in X,Y, and in Z. The integration is illustrated in Fig. 5. The second of the three summations is necessary since particle positions may have to be interpolated to intermediate positions during a time step to avoid missing grid points if the cylinder radius is smaller than the advection distance.

3. METEOROLOGY

Spatial and temporal density of the input meteorology is probably one of the most important factors controlling the advection and dispersion calculations. The HY-SPLIT code was designed to use previously gridded data in synoptic (time series) format. There are two options: (1) data are available only at rawinsonde and surface observation points or (2) data have already been gridded. For option 1 a preprocessor program is available to grid the data as required. For option 2 the gridded data are processed by a routine within HY-SPLIT to compute the necessary diagnostic variables required for dispersion and advection calculations--in particular vertical velocity and the vertical mixing coefficient profiles over the entire model domain. In this section the gridded data are assumed to be as provided by the NWS Nested Grid Model (Phillips, 1975). The initial fields and forecasts to 12 h are archived in series to generate a diagnostic data set; however, 48-h forecasts are available on an operational basis if dispersion forecasts are required.

3.1 Rawinsonde and Surface Data

The meteorological preprocessor generates a time series of gridded observations. Rawinsonde data above an observation point are first linearly interpolated at the designated vertical grid resolution to the top of the model at the nearest horizontal grid point. Wind direction and speed are converted to components relative to the polar stereographic grid. Temperature and pressure are directly interpolated to the vertical grid while dewpoint is first converted to wet bulb potential temperature and then interpolated to the grid. While the complete original sounding is available, the top of the mixing depth is estimated to be the height of the base of the first elevated temperature inversion (Heffter, 1980). This value is used later to scale the vertical-mixing-coefficient profile.

At this point the sounding is further analyzed to determine the stability. The method follows that of Pielke and Mahrer (1975) in which equations for the Monin-Obukhov length, friction velocity, and surface friction potential temperature are solved by iteration using the surface layer flux relations of Businger (1973). After the stability is calculated, the K_z profile is determined using the interpolation formula of O'Brien (1970). All the relevant equations and calculation procedures have been outlined by Draxler (1986).

After all the rawinsonde measurements are processed and assigned to the grid point nearest to the observation site, the data at the remaining grid points are interpolated from the grid points containing the rawinsonde data, using a conventional weighting (inverse distance squared). From rawinsonde

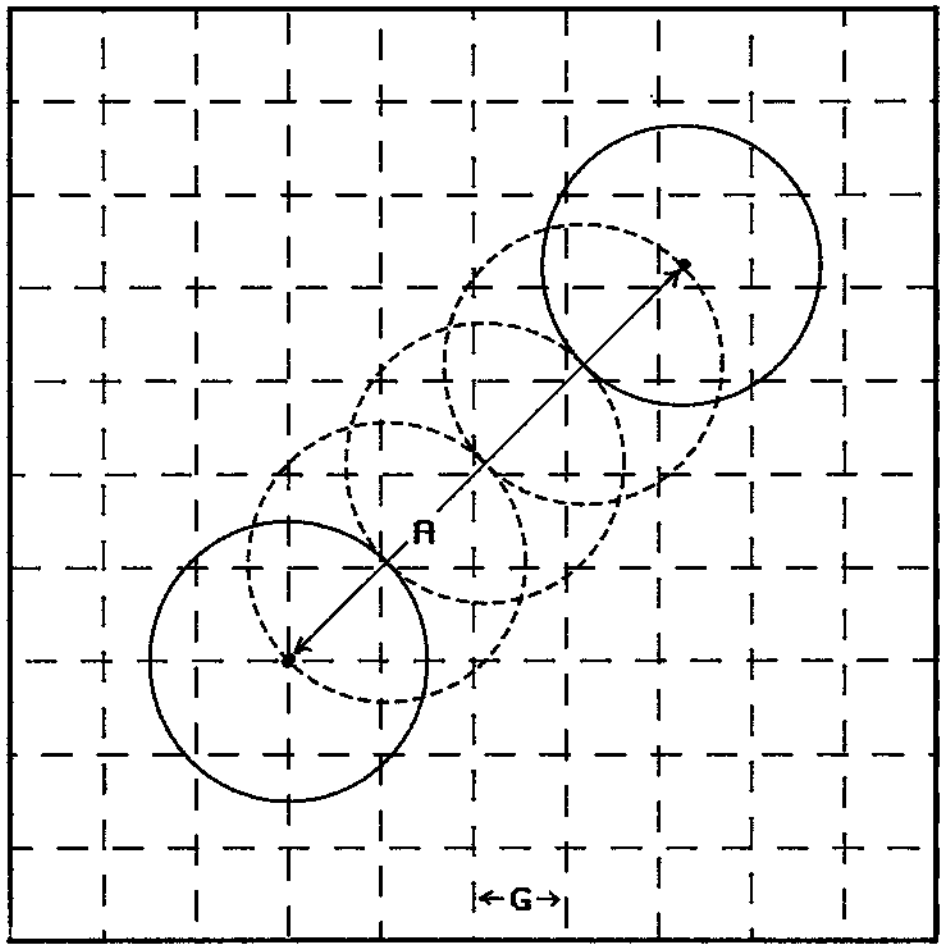

Figure 5. The distance a particle is advected (A) during a time step. Three intermediate particle positions are interpolated so that concentrations can be computed at all grid points within the interpolated circles (dashed) as well as within the initial and final positions (solid).

observations taken either every 6 or 12 h, the gridded data are then linearly interpolated at intermediate intervals as frequently as desired.

If surface observations are available, an additional step can be implemented. Because the surface data are taken each hour over a much denser spatial network, these data can be used in a variety of ways. One of the most uncertain aspects of the model calculation is the temporal variation of the vertical mixing coefficient between two daily rawinsondes. When surface observations are available, as the interpolated fields are calculated, the lowest level interpolated temperature is replaced by the surface temperature observation. The stability is then recomputed as before, and new vertical mixing profiles are calculated.

After the meteorological data are gridded at each interpolation time, vertical motions are estimated by assuming that the wet-bulb potential temperature θ_w is conserved during an air parcel's ascent (Byers, 1974; p. 132). This method is preferred over integrating the velocity divergence because small errors in rawinsonde derived winds can produce large errors in the divergence field. Therefore, following the motion along a trajectory, the total derivative of θ_w is zero and hence the local rate of change is due only to advection. If we ignore the diabatic effects in the boundary layer and assume the θ_w field is frozen in time for the duration of the transport model advection time step, then the vertical velocity is

$$W = \left(- U \frac{\partial \theta_w}{\partial x} - V \frac{\partial \theta_w}{\partial y}\right)\left(\frac{\partial \theta_w}{\partial z}\right)^{-1} .$$

In this case, W is the vertical velocity required to maintain an air parcel on the same θ_w surface as computed at each grid point at a particular observation time. Applying this vertical velocity will not result in true isentropic flow as defined by Danielson (1961), for it is based only upon the slope of the θ_w surface with no energy constraints. However in the boundary layer, isentropic trajectories are frequently in error since $\partial\theta_w/\partial z$ approaches zero in a well-mixed atmosphere. The primary purpose of defining W in this way is to permit particle trajectories to maintain a more realistic flow near air mass boundaries, where large horizontal and vertical gradients of θ_w make the calculation of W more accurate. When the gradients are calculated, one value of $\partial\theta_w/\partial z$ is computed below and one above the mixed layer by a least-squares linear regression of θ_w on height. The vertical velocity is then integrated to each level from the appropriate average value of $\partial\theta_w/\partial z$ and the centered difference horizontal gradients. If the value of $\partial\theta_w/\partial z$ is less than $0.001°K\ m^{-1}$, then a well-mixed layer is assumed and W is set to zero.

The final output of the meteorological preprocessor then contains gridded fields of U, V, W, θ_w, T, and K_z, at user-specified heights and time intervals.

3.2 NWS-NGM Gridded Data

The NGM model forecast is initialized every 12 h (0000 and 1200 GMT), and the forecast fields are calculated to 48 h. ARL archives the initial fields and each forecast field out to 12 h, when a new initial field becomes available. The output interval of the forecast fields can vary from 1 to 6 h. The archived model output can be available on as many as 16 sigma surfaces at the midpoints

of layers that vary in thickness from 35 mb at the surface to 54 mb at the model top. The routine archive includes the three-dimensional state variables:

U, east/west wind speed
V, north/south wind speed
T, temperature
S, specific humidity.

The diagnostic vertical velocity W is optional. If not available, it is computed in HY-SPLIT from the vertical integration of the horizontal velocity divergence. In addition the two-dimensional variables are archived:

P_0, surface pressure (mb)
F_h, sensible heat flux at the surface (W m^{-2})
F_m, surface momentum exchange (kg m^{-2} s^{-1})
Z_{bl}, mixed layer depth (m).

Although other variables are also available, only these will be discussed here because they are used to develop the mixing-coeffient profile used in the dispersion calculations.

At each grid point the hydrostatic equation

$$dZ = -dP/\rho g$$

is integrated to convert the model layers defined at sigma surfaces to heights using the local virtual temperature

$$T_V = T/(1 - 0.6S)$$

to compute the air density

$$\rho = M\ R^{-1}\ T_V^{-1}$$

where R is the universal gas constant, and M is the molecular weight of air. Then the surface and first-sigma-level parameters are used to compute the Monin-Obukhov length

$$L = u_*^2\ T_V/k\ g\ \theta_*\ ,$$

where Von Karman's constant k is assumed to be 0.4 and the friction potential temperature

$$\theta_* = -F_h/\rho C_p\ u_*.$$

Here C_p is defined as the specific heat at constant pressure and the surface friction velocity

$$u_*^2 = F_m\ u_1/\rho_1,$$

where the scalar velocity u and air density are at the first sigma level. It is assumed that the height of the constant flux layer Z_s equals 0.25 Z_1, and then at the top of the surface layer the vertical mixing coefficient

$$K_Z = k u_* Z_s / \phi .$$

The normalized velocity profiles ϕ are taken from Businger (1973) such that when

$$L < \phi \quad : \quad \phi = (1 - 16\ Z_s/L)^{-0.25}$$

and when

$$L > \phi \quad : \quad \phi = (1 + 4.7\ Z_s/L).$$

Two methods are used to calculate the vertical-mixing-coefficient profile. In the first method, similar to the method discussed in section 3.1, the O'Brien (1970) interpolation formula is used to derive the K_Z profile to the top of the mixed layer. Above the mixed layer top to the top of the model, a small value of 0.1 $m^2\ s^{-1}$ is used for K_Z. These calculations are very similar to those used for rawinsonde data, except it is not necessary to solve the surface layer flux relations by iteration. The second method is introduced to incorporate local stability measures above the mixed layer. Because the above technique applies only to turbulence generated by a boundary layer from surface-based momentum and heat flux values, a bulk Richardson number

$$Ri = g \frac{d(\ln \theta)/dz}{(du/dz)^2}$$

is calculated for each sigma level. Following the technique used in the NGM model calculation (Phillips, 1986), a vertical mixing coefficient is calculated assuming an arbitrary maximum value of 30 $m^2\ s^{-1}$ so that

$$K_Z = 30/(1 + |Ri|).$$

The final K_Z value at any grid point is the maximum value obtained from either of the two methods. In this way, if significant wind-shear-induced turbulence is generated at night or above the boundary layer, the particle dispersion calculation will reflect the appropriately higher mixing rate.

4. MODEL OUTPUT OPTIONS

HY-SPLIT calculation results can be displayed on a printer or high resolution graphics terminal at any user-selected height or time interval. Two basic output data are provided: maps of particle positions and maps of air concentrations. Concentrations can be output at a specific data level, or by indicating a range of levels, the concentrations will be layer averaged over that range. The air concentration maps can be printed or can be saved on a mass storage medium. The concentration data can also be displayed on a graphics terminal in map form, also at a particular level or averaged over several levels and cross-sectional vertical profiles. The input data required to generate the following examples are given in section 5.

4.1 Printer Maps

Particle position maps are snapshots, as the particle trajectories are not saved. The date and time in the upper left corner of the sample shown in Fig. 6 gives the time of the snapshot. The projection is polar stereographic and the display window (latitude and longitude - line 18) are user selectable. The origin location (line 9) is indicated by the asterisk and the position of each particle is represented by a number indicating the maximum sigma level reached by any particle in that print position. In this illustration the source has been a continuous one for several days (line 12).

An example of grid point concentrations for the 24-h period preceding the snapshot map in Fig. 6 is given in Fig. 7 for concentrations at a height of 1 m. Other heights and ranges can be selected in the input section (line 14 and line 15). Concentrations are represented by three digits; the central digit is located over the grid point. The first digit is the mantissa, the second and third the negative exponent. For example, 311 would be interpreted as a concentration of 3×10^{-11} mass units per cubic meter. Notice the regions of concentration are larger than the corresponding particle positions. The reason for this is that the concentrations are 24-h averages and the particle positions are shown only at the end of the sampling period as indicated by the time in the upper left corner of the map.

4.2 Graphics Display

High-resolution graphics output is generated for display on a Tektronics terminal. The concentration map for the same case as in Figs. 6 and 7 is shown in Fig. 8. The map time is indicated in the lower left corner, and the large panel shows the same concentration field as in Fig. 7 with contours automatically selected at natural log intervals. The contours are marked by the negative natural log of the concentration. For example contour "30" near Lake Michigan would be the 9×10^{-14} mass m^{-3} contour. The lower and left side panels show the vertical crosswind integrated concentration profiles in the east-west and north-south grid directions, respectively. Concentrations are integrated in the direction normal to the display, the top height corresponding to the maximum height selected by the user (line 14). Contour numbering is the same as for the horizontal display except units are in mass per square meter.

5. MODEL INPUT SAMPLE

There are eighteen input lines required to initialize a model simulation. Individual computer installations may require modification of the methods used to pass variable dimension sizes. Otherwise standard Fortran-77 conventions are used for list directed input. Default settings are provided for all input lines and are selected by returning a line feed "/". The default values for the example in Figs. 6-8 are shown on each line. Input lines 2 through 6 refer to the grid illustrated in Fig. 9.

Line 1: 190.5 60.0 27.0 49.0 105.0

Meteorological grid spacing (km), which is true at latitude (deg), north pole X coordinate, north pole Y coordinate, with the grid parallel to longitude (deg).

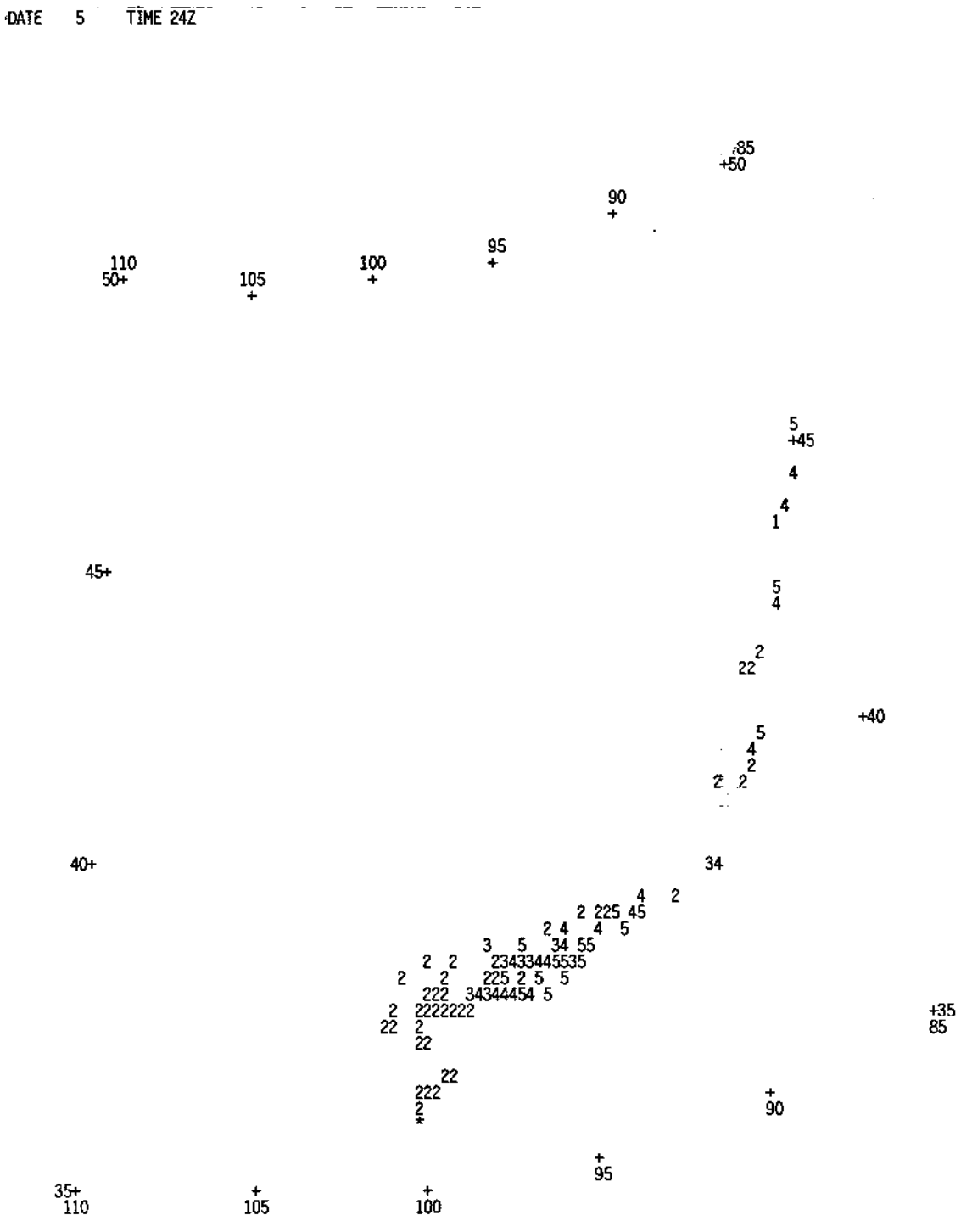

Figure 6. Standard printer particle position map. Each single digit indicates the sigma level (1 = lowest) or the highest particle at that print position. The asterisk indicates the source location; the values with the pluses indicate latitudes and longitudes (deg).

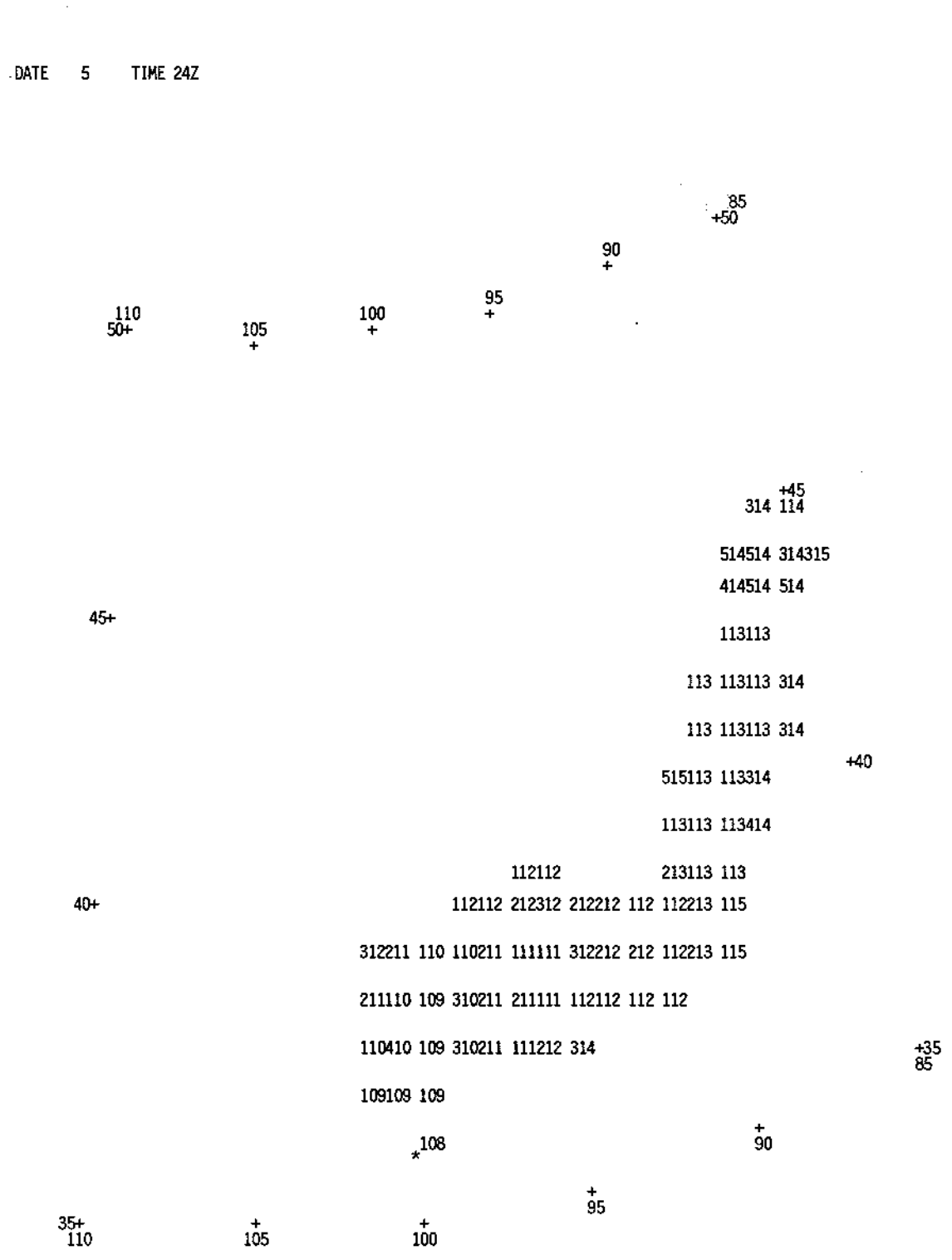

Figure 7. Standard printer concentration map. The three-digit concentrations give the mantissa and exponent such that a 212 would be a concentration of 2 x 10^{-12} units m^{-3}. The asterisk indicates the source location; the values with the pluses indicate latitudes and longitudes (deg).

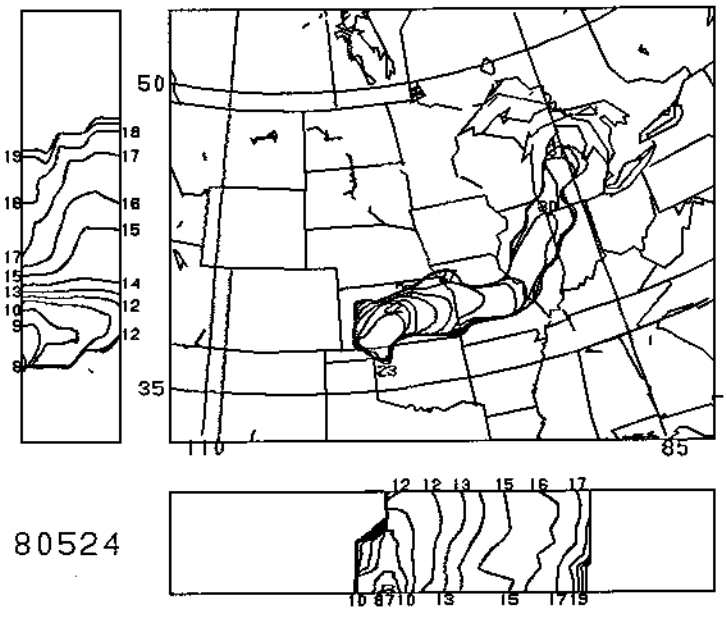

Figure 8. Contoured concentration fields from the high-resolution graphics output option. Plane view at the heights selected in the input section as well as east-west (bottom) and north-south (left) cross sections are shown. Contour units are in negative natural log of concentration (m^{-3} in plane and m^{-2} for the cross section). Map backgrounds are generated by the display program. The time (month, day, hour) is at the lower left.

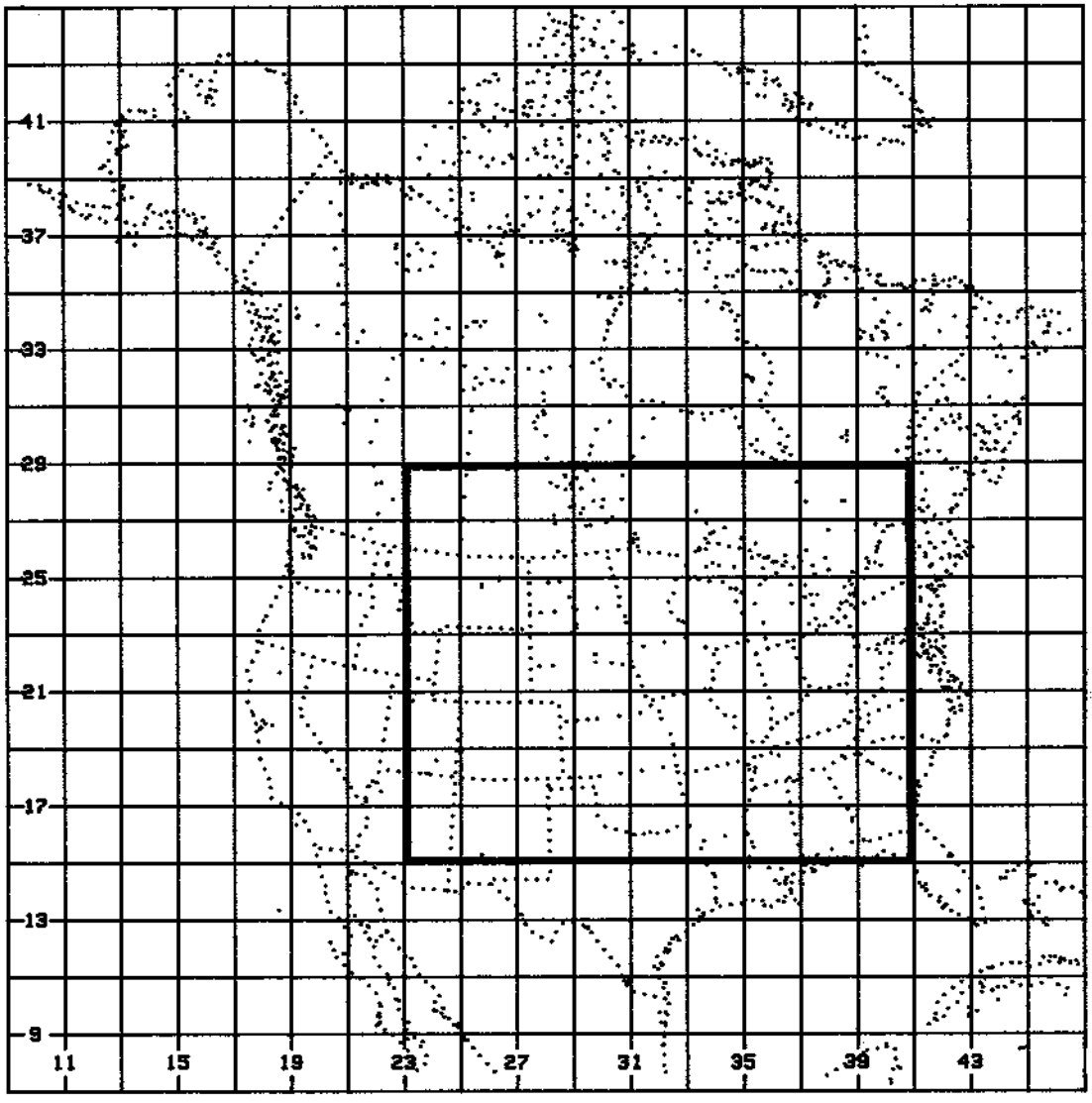

Figure 9. Meteorological grid used in example calculations. Every other grid point is shown. The subgrid indicated by the bold lines is the concentration and map subgrid selected for the examples in Figs. 6, 7, and 8.

Line 2: 9 47 7 45 5

X-low, X-high, Y-low, Y-high, K-high -- the upper and lower limits of the meteorological grid used in all variable dimensions.

Line 3: 2.0

M-grid/C-grid -- the ratio of the meteorological grid spacing to the concentration grid spacing. The default value indicates that there are two concentration grid points for each meteorological grid point.

Line 4: 23 59 15 43 9

X-low, X-high, Y-low, Y-high, K-high -- the upper and lower limits for the variable dimensions of the concentration grid where X-low, Y-low must be coincident with the meteorological grid. This grid is illustrated by the bold subgrid in Fig. 9. One can picture the lower left corner of the concentration grid fixed, and the grid would expand or contract depending upon the ratio defined in line 3. The upper right corner can be located in meteorological grid coordinates by computing: (high-low)/(line 3) + low.

Line 5: 3 6

The advection time step (h), and the interval at which meteorological input data are available (h) from NGM or rawinsonde gridding preprocessor.

Line 6: 1.0

Fraction of the particle cylinder radius used to determine which particles are to be merged (see section 2.4, Fig. 4).

Line 7: 8 4 0

The simulation start time by month, day, and hour.

Line 8: 2

The number of days for the simulation.

Line 9: 36.0 100.0 25.0

The latitude (deg), longitude (deg), and height (m) of the particle source location.

Line 10: 0

The particle initialization index -- 0, none; 1, read positions saved on disk (FORTRAN unit number 14) from last simulation; 2, write particle positions at the end of the simulation; 3, read as in (1) and write as in (2).

Line 11: 1000.0

The emission rate at origin point in mass units per hour.

Line 12: 48

The number of hours of emission. This should be larger than or equal to the total simulation time (line 8) for a continuous source, but not less than the time step (line 7).

Line 13: 24

The number of hours concentrations are to be averaged. This number is also the output interval for position and concentration maps.

Line 14: 1 300 600 900 1200 1500 1800 2100 2400

The heights (m) of each concentration calculation level. There should be K-high (line 4) entries on this line.

Line 15: 1 1

K-low, K-high -- the vertical grid index values of the horizontal planes that will be averaged and displayed for concentration maps. There are K-high (line 4) possible index values.

Line 16: 0

The disk output index for concentrations -- 0, none; 1, read only previously calculated concentrations; 2, initialize file and start writing at the beginning; 3, modify the file by writing to the end. The entire concentration array is saved at the averaging interval (line 13) to FORTRAN unit number 12.

Line 17: 1 1 1

Concentration map flag, particle position map flag, and graphics maps flag -- 0, no maps; 1, maps at the interval specified (line 13).

Line 18: 50.0 35.0 110.0 85.0 5.0

Top latitude, bottom latitude, left longitude, right longitude, and the lat/lon interval are the ranges for the labels that will be placed on all output maps at the degree interval specified.

6. REFERENCES

Businger, J.A., 1973: Turbulent transfer in the atmospheric surface layer. Workshop on Micrometeorology, August 14-18, 1972, D.A. Haugen (Ed.), Amer. Meteorol. Soc., Boston, MA, 67-100.

Byers, H.R., 1974: General Meteorology. McGraw-Hill, New York, 461 pp.

Danielson, E.F., 1961: Trajectories: Isobaric, isentropic, and actual. J. Meteorol., 18, 470-486.

Draxler, R., 1982: Measuring and modeling the transport and dispersion of Kr-85 1500 km from a point source. Atmos. Environ., 16, 2763-2776.

Draxler, R., 1986: Simulated and observed influence of the nocturnal urban heat island on the local wind field. J. Clim. Appl. Meteorol., 25, 1126-1137.

Draxler, R., 1987: Sensitivity of a trajectory model to the spatial and temporal resolution of the meteorological data during CAPTEX. J. Clim. Appl. Meteorol., 26, 1577-1588.

Draxler, R., and B.J.B. Stunder, 1988: Modeling the CAPTEX vertical tracer concentration profiles. J. Appl. Meteorol., 27, 617-625.

Draxler, R., and A.D. Taylor, 1982: Horizontal dispersion parameters for long-range transport modeling. J. Appl. Meteorol., 21, 367-372.

Heffter, J.L., 1965: The variation of horizontal diffusion parameters with time for travel periods of one hour or longer. J. Appl. Meteorol., 4, 153-156.

Heffter, J.L., 1980: Transport layer depth calculations. Second Joint Conf. on Applications of Air Pollution Meteorology, March 24-27, 1980, New Orleans. Amer. Meteorol. Soc., Boston, MA, 787-791.

Hunt, J.C.R., 1985: Diffusion in the stably stratified atmospheric boundary layer. J. Clim. Appl. Meteorol., 24, 1187-1195.

Lange, R., 1978: ADPIC--A three dimensional particle-in-cell model for the dispersal of atmospheric pollutants and its comparision to regional tracer studies. J. Appl. Meteorol., 17, 320-329.

O'Brien, J.J., 1970: A note on the vertical structure of the eddy exchange coefficient in the planetary boundary layer. J. Atmos. Sci., 27, 1213-1215.

Phillips, N.A., 1975: The Nested Grid Model. NOAA Technical Report NWS-22, U.S. Department of Commerce, Silver Spring, MD, 80 pp.

Phillips, N.A., 1986: Turbulent mixing near the ground for the Nested Grid Model. Office Note 318, National Meteorological Center, National Weather Service, Silver Spring, MD, 19 pp.

Pielke, R.A., and Y. Mahrer, 1975: Representation of the heated planetary boundary layer in mesoscale models with coarse vertical resolution. J. Atmos. Sci., 32, 2288-2308.